

P.-H. PIOGER^{1,✉}
V. COUDERC¹
L. GROSSARD¹
A. BARTHÉLÉMY¹
F. BARONIO²
C. DE ANGELIS²
Y.H. MIN³
V. QUIRING³
W. SOHLER³

Ultra-fast reconfigurable spatial switching between a quadratic solitary wave and a weak signal

¹ XLIM, Faculté des Sciences, Université de Limoges/CNRS, 123 Ave. A. Thomas, 87060 Limoges, France
² Dipartimento di Elettronica per l'Automazione, Università di Brescia, via Branze 38, 25123 Brescia, Italy
³ Universität Paderborn, Angewandte Physik, 33095 Paderborn, Germany

Received: 7 March 2006/Revised version: 24 May 2006
Published online: 28 June 2006 • © Springer-Verlag 2006

ABSTRACT Experimental and numerical investigations of an ultra-fast reconfigurable spatial switch based on the nonlinear interaction between a weak wave (the signal) and a solitary wave (the control) at 1548 nm are reported. The non-collinear interaction in a quadratic nonlinear film waveguide gives birth to a third switched optical beam (the idler). This beam could be steered according to the transverse spatial position of the control beam.

PACS 42.65.Ky; 42.65.Re; 42.65.Wi

1 Introduction

Nowadays, the most important drawback of the telecommunication systems is the data-rate processing and routing, which is currently limited by electronic systems. The speed of these systems is restricted by the double conversion between optical signals and electrical signals. Self-guided optical beams, in particular quadratic spatial solitons, are theoretically and experimentally studied for their potential application to ultra-fast all-optical switching and routing [1, 2].

Quadratic spatial solitons (QSSs) consist of multifrequency waves strongly coupled by second-order nonlinearity; QSSs result from the mutual trapping and locking of the beams at the fundamental frequency (FF) and at the second-harmonic frequency (SH) through parametric interactions. These types of solitary waves are stable and robust in guided and bulk geometries. Numerical and experimental investigations have already demonstrated the possibilities offered by QSSs to realize all-optical addressing devices by soliton collision in one and two dimensions. Repulsion, fusion, spiraling, and spatial steering of QSSs were already demonstrated and studied [3–11]. In most of these configurations, the operations of ultra-fast switching exploited two spatial solitons which required high peak powers.

In this paper, we present a reconfigurable spatial switching that results from a non-collinear interaction between a quadratic spatial soliton (FF and SH waves) and a weak FF wave propagating in a periodically poled Ti-indiffused

lithium niobate (Ti:PPLN) film waveguide. The principle of this ultra-fast reconfigurable switch is based on the parametric interaction between the weak beam (the signal) and the strong SH component of the soliton beam (the control). Difference-frequency generation (DFG) between these two waves generates a third wave (the idler) at the fundamental wavelength in a direction that satisfies the wave-vector phase-matching condition. The output position of the switched signal can be steered by varying the transverse position where the control beam is launched into the waveguide. The paper is organized as follows. In Sect. 2 we report the experimental set-up of the switching mechanism. We present in Sect. 3 the numerical model used to simulate the interaction between the signals. In Sect. 4 we report the main experimental and numerical results. Finally, in Sect. 5 we draw our conclusions.

2 Experimental set-up

The experimental set-up used for the spatial switching is shown in Fig. 1. The all-fibre laser source delivers pulses with a Gaussian temporal profile and a pulse width of 4 ps with a repetition rate of 20 MHz. The spectrum of the emitted pulses is centred at 1548 nm with a 2.2-nm spectral width (FWHM in intensity). This FF beam is split into two waves in a Michelson-type interferometer. The relative spatial position and propagation direction of the two beams can be modified by the misalignment of one arm of the interferometer. The temporal delay between the two signals can also be modified by changing the length of one arm. The two waves are then focused onto the entrance face of a 63-mm-long (L) lithium niobate film waveguide; by means of a telescope the waves are shaped into a highly elliptical spot, nearly Gaussian in profile, with a FWHM in intensity of 56 μm along the non-guided dimension and 3.9 μm along the perpendicular direction. The 4- μm -thick planar waveguide is fabricated in a Z-cut substrate by indiffusion of a 70-nm-thick, vacuum-deposited Ti layer at 1060 °C. The thickness of the waveguide permits the propagation of a single TM₀ mode of 4- μm width at the FF; several TM modes are supported at the SH, but only the TM₀ of 3- μm width is efficiently pumped by the TM₀ at the FF. A uniform micro-domain structure of periodicity $\Lambda = 16.9 \mu\text{m}$ (duty cycle 0.5) has been generated after waveguide fabrication by electric-field-assisted poling. The sample

✉ Fax: +33-555457253, E-mail: paul-henri.pioger@xlim.fr

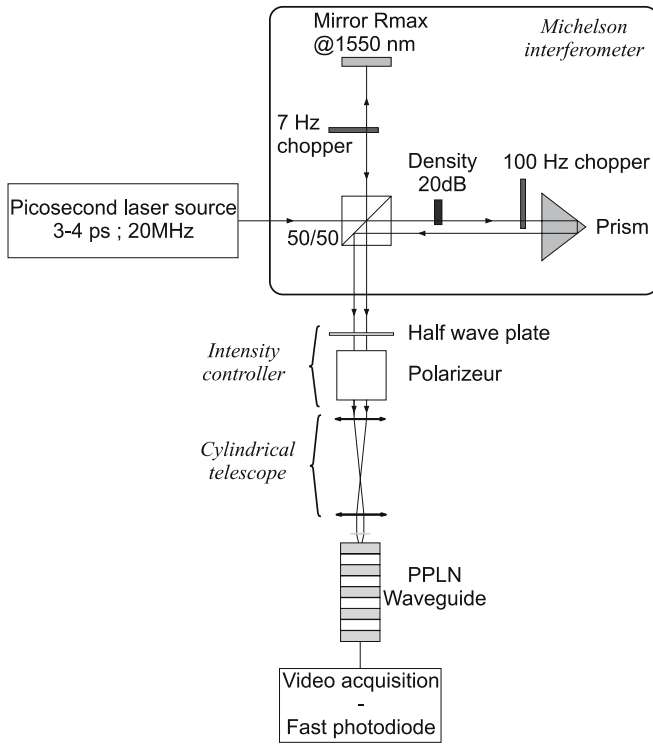


FIGURE 1 Experimental set-up used for non-collinear spatial switching process in Ti:PPLN waveguide based on a Michelson interferometer

is inserted in a temperature-stabilized oven and operated at elevated temperature (120–160 °C) to reduce photorefractive effects. Phase-matching conditions can be modified by tuning the temperature.

In this configuration, the signal beam consists of 4-ps pulses at a repetition rate of 20 MHz, modulated by a mechanical chopper at a frequency of 100 Hz, with a duty cycle equal to 0.55. The intensity of the signal, adjusted by a density filter placed on one arm of the interferometer, is roughly 100 times lower than that of the control beam. The control beam (both FF and SH components) is obtained by launching an intense FF wave and exploiting SH generation in the PPLN crystal. The control beam consists of 4-ps pulses at a repetition rate of 20 MHz, modulated by a rectangular signal at a frequency of 7 Hz (duty cycle = 0.9). These mechanical modulations permit us to well differentiate the signal and the control components for experiments. The two beams are launched simultaneously into the waveguide and cross inside with variable angle and phase difference. The control-beam intensity is sufficiently high to excite a soliton beam during the propagation in the Ti:PPLN crystal. In the solitary wave propagation conditions, the SH wave is spatially and temporally locked and superimposed with the FF component, thus mitigating the effect of group-velocity mismatch (GVM). Note that the phase-mismatch conditions should be positive enough to allow the spatial soliton propagation ($\Delta kL > 8\pi$) [12, 13]. Moreover, the excitation of a spatially trapped beam permits us to compensate the divergence of the control beam and therefore to separate more efficiently the beams (signal, control, and idler) at the output face of the crystal. The output signals were recorded and analysed with a vidicon camera and a fast photodiode.

3 Numerical modelling

We model the electric fields E_1 at the fundamental wavelength ω_0 (FF), and E_2 at the second harmonic $2\omega_0$ (SH), with $\omega_0 = 2\pi c/\lambda_0$ and $\lambda_0 = 1548$ nm free-space wavelength propagating in the y direction, as

$$E_1(x, y, z, t) = \frac{1}{2}(m_1(z)a_1(x, y, t) \exp(-j[\beta_{\omega_0}y + \omega_0t]) + \text{c.c.}),$$

$$E_2(x, y, z, t) = \frac{1}{2}(m_2(z)a_2(x, y, t) \exp(-j[\beta_{2\omega_0}y + 2\omega_0t]) + \text{c.c.}).$$

Here, $m_1(z)$ and $m_2(z)$ are the mode profiles at the FF and SH in the guided dimension; $a_1(x, y, t)$ and $a_2(x, y, t)$ are the slowly varying envelopes. Averaging over the quasi phase matching periods, at the lowest order, $a_1(x, y, t)$ and $a_2(x, y, t)$ obey the nonlinear coupled equations

$$j \frac{\partial a_1}{\partial y} - j\beta'_{\omega_0} \frac{\partial a_1}{\partial t} - \frac{\beta''_{\omega_0}}{2} \frac{\partial^2 a_1}{\partial t^2} + \frac{1}{2\beta_{\omega_0}} \frac{\partial^2 a_1}{\partial x^2} + \frac{\chi^{(2)}\omega_0}{2cn_{\omega_0}} \times \frac{\int m_2|m_1|^2 dz}{\int |m_1|^2 dz} a_2 a_1^* e^{-j\Delta kz} = 0,$$

$$j \frac{\partial a_2}{\partial y} - j\beta'_{2\omega_0} \frac{\partial a_2}{\partial t} - \frac{\beta''_{2\omega_0}}{2} \frac{\partial^2 a_2}{\partial t^2} + \frac{1}{2\beta_{2\omega_0}} \frac{\partial^2 a_2}{\partial x^2} + \frac{\chi^{(2)}\omega_0}{2cn_{2\omega_0}} \times \frac{\int m_2|m_1|^2 dz}{\int |m_2|^2 dz} a_1^2 e^{j\Delta kz} = 0, \quad (1)$$

where β represents the propagation constant, β' the inverse group velocity, and β'' the inverse group-velocity dispersion; n is the refractive index, $\Delta k = 2\beta_{\omega_0} - \beta_{2\omega_0} + K_S$, where $K_S = 2\pi/\Lambda$, and $\chi^{(2)} = 2/\pi \chi_{zzz}^{(2)}$ is the nonlinear coefficient. We employ a finite-difference vectorial mode solver to determine the linear propagation properties in the slab waveguide; finally, we solve the nonlinear coupled equations using a finite-difference beam-propagation technique.

The crystal length L of the Ti:PPLN waveguide corresponded to 5.6 times the diffraction length associated with the FF input beam (56 μm FWHM). In the temporal domain, the length is equivalent to 5.2 times the group velocity mismatch length between FF and SH components of the trapped beam (pulse duration = 4 ps FWHM). The dispersive terms can be neglected.

4 Results

In the numerical simulations and experiments, the two input waves (signal and control) were focused on the input face of the waveguide with an angle of 0.5° between the two directions of the two waves in the PPLN crystal. The beams are superimposed in the nonlinear medium a few millimetres inside the waveguide. The modulations of the signal and control beams at the input are shown in Fig. 2a and b. Through the DFG interaction between the SH component of the control beam and the signal at the FF, we succeeded in obtaining a switched idler signal at the FF (Fig. 2c). After the propagation, the signal and control beams keep their own

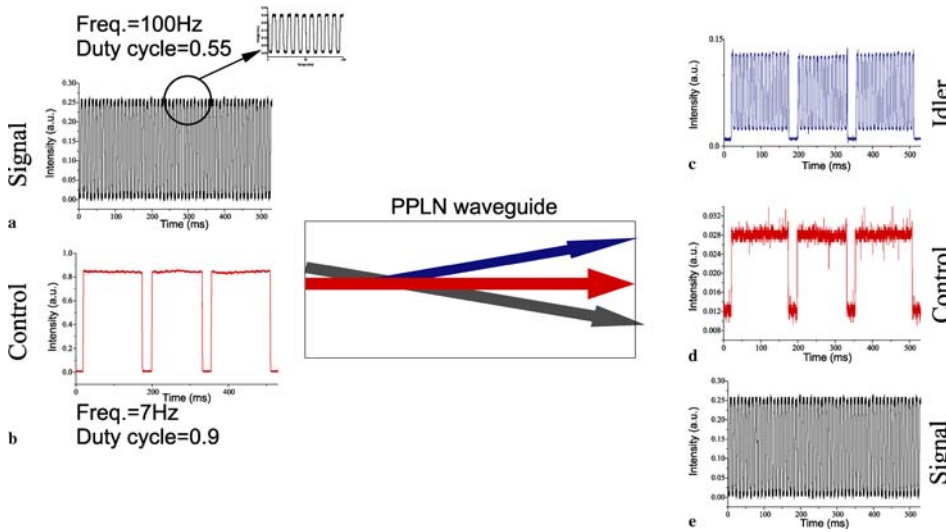


FIGURE 2 Experimental results of the non-collinear switching device. (a) Input signal beam at FF, frequency modulation = 100 Hz, duty cycle = 0.55; (b) input control beam at FF, frequency modulation = 7 Hz, duty cycle = 0.9; (c) output idler switched beam at FF characterized by both signal and control modulations; (d) output control beam at FF; (e) output signal beam at FF

modulation (see Fig. 2d and e). Regarding the switched beam (idler), the signal recorded by the photodiode represents both the weak input beam modulation and control beam's one. The switched wave was spatially filtered by an aperture before detection. It carried pulses of 0.18-W peak power for a FF control peak power of 1500 W and for an input signal of 15 W. The efficiency of the spatial switching (-19 dB) depended on the space-time overlap between the two input beams; it could be improved with a reduction of the angle between signal and control and a longer waveguide. The contrast in the switched output was higher than 14 dB with reference to the non-switched pulses.

In the collinear regime, i.e. when the two input beams propagate in the same direction with a perfect overlapping, the DFG can occur only for a fixed phase difference between the two waves. The phase relation leading to a maximum efficiency of conversion is $\pi/2$. On the contrary, in non-collinear geometry, the spatial superimposition of the beams generates interferometer fringes leading to several spatial positions where DFG conditions are respected. In this case the variation of the phase difference between the input waves leads only to a spatial translation of the fringes. In the case of a sufficiently high angle between the propagation directions of the two waves, DFG conditions can be respected. For a sufficient number of fringes, the DFG efficiency is quasi-insensitive to the phase difference between the two input beams, and in consequence to the transverse position of the control beam. In fact, owing to the non-degeneracy of the parametric process the switching is phase insensitive [14]. In this sense the presented system is an ultra-fast reconfigurable spatial switching device. The conversion efficiency of the idler wave, which represents the switched signal, stays low but with quasi-constant energy.

Numerical results showing the capability of processing weak signals, that correspond to the above-mentioned experiments, are presented in Fig. 3. We plotted the spatial profiles of the beams at the output face of the PPLN waveguide for two input signal phase differences (Fig. 3a: phase difference = π , Fig. 3b: phase difference = 0). For both cases, the idler beam is generated inside the crystal and can be observed at the output face. It is clearly shown that the impact of the phase

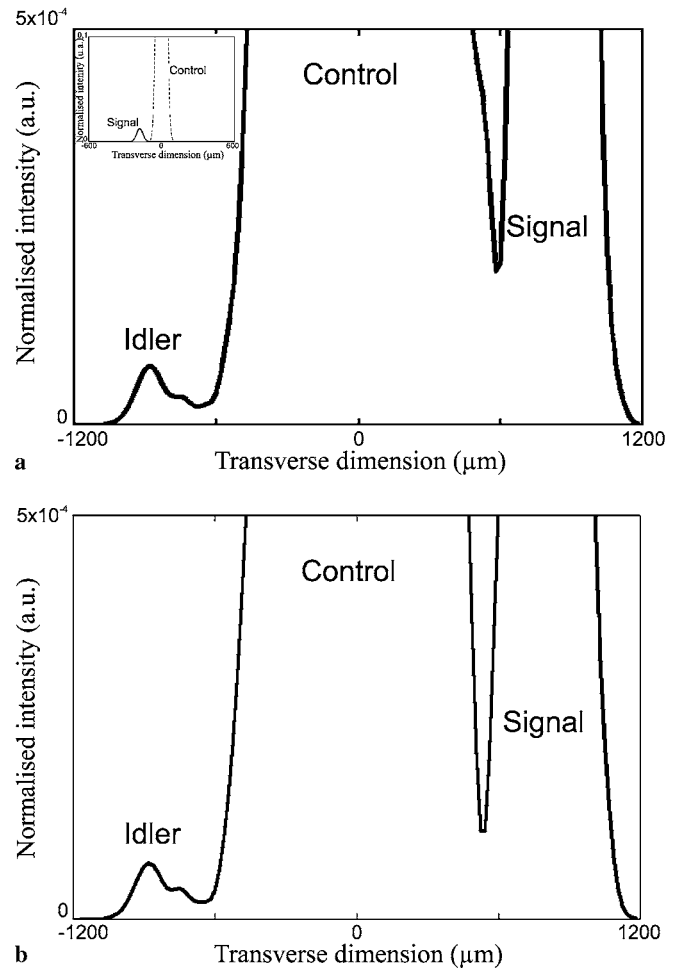


FIGURE 3 Numerical spatial output profiles of the idler, control, and signal beams. (a) The control-signal phase difference is equal to π . (b) The control-signal phase difference is equal to 0. The inset in (a) shows the input spatial profiles of the signal wave and the control wave. The y axis in the plots has been zoomed in to better show the shape of the weak switched signal

difference between the input waves has a low impact on the switched signal profile and amplitude. The y axis in the plots in Fig. 3 has been zoomed in to better show the shape of the weak switched signal. The input beams' spatial positions and

profiles are shown in the inset of Fig. 3a. We do not notice a significant modification of the conversion efficiency, neither of the output spatial profiles. As already mentioned, the output position of the switched signal can be tuned by changing the relative propagation direction of the two waves and the crossing point position in the PPLN. Thus, the output position of the switched signal can be steered according to the transverse position of the control beam.

In this configuration, the main limitation in terms of repetition rate is due to the GVM between the fundamental frequency and the second-harmonic waves. Nevertheless, in the present case, the temporal second-harmonic walk-off effect was compensated by the quadratic space–time locking of the fundamental and second-harmonic control [13]. This temporal locking between the FF and the SH components of the control beam increases the capability of this device to operate at very high bit rates, around 125 Gb/s for a pulse duration equal to 4 ps. It could also allow simultaneous spatial switching and frequency conversion by using a control wave detuned in frequency with respect to the signal wave.

5 Conclusion

We presented an ultra-fast reconfigurable spatial switch based on the non-collinear interaction of a weak signal wave and a control wave in a Ti:PPLN waveguide. The signal beam was a weak 4-ps pulse at 1548 nm with a peak power equal to 15 W; the control beam was a quadratic solitary wave at 1548 nm. The principle of the ultra-fast reconfigurable switch is based on the parametric interaction between the signal and the control. Difference-frequency generation between these two waves generates an idler wave

at 1548 nm, the switched signal. Experiments and numerical results show that the switching system is insensitive to the phase difference between the input waves. Thanks to the non-collinear interaction of the beams, no significant modification of the switched wave has been observed. This system could be used with independent sources. Moreover, the output position of the switched signal can be steered by varying the transverse position where the control beam is launched into the waveguide. This ultra-fast addressing system presents an interesting all-optical method of weak signal switching.

REFERENCES

- 1 Y.N. Karamzin, A.P. Sukhorukov, JETP Lett. **20**, 339 (1974)
- 2 W.E. Torruellas, Z. Wang, D.J. Hagan, E.W. Vanstryland, G.I. Stegeman, L. Torner, C.R. Menyuk, Phys. Rev. Lett. **74**, 5036 (1995)
- 3 W.E. Torruellas, G. Assanto, B.L. Lawrence, R.A. Fuerst, G.I. Stegeman, Appl. Phys. Lett. **68**, 1449 (1996)
- 4 G. Leo, G. Assanto, J. Opt. Soc. Am. B **14**, 3151 (1997)
- 5 V.V. Steblina, Y.S. Kivshar, A.V. Buryak, Opt. Lett. **23**, 156 (1998)
- 6 R. Schiek, Y. Baek, G.I. Stegeman, W. Sohler, Opt. Quantum Electron. **30**, 861 (1998)
- 7 A. Buryak, P. Di Trapani, D. Skryabin, S. Trillo, Phys. Rep. **370**, 63 (2002)
- 8 A.V. Buryak, V.V. Steblina, J. Opt. Soc. Am. B **16**, 245 (1999)
- 9 P.H. Pioger, F. Baronio, V. Couderc, A. Barthélémy, C. De Angelis, Y. Min, V. Quiring, W. Sohler, IEEE Photon. Technol. Lett. **16**, 560 (2004)
- 10 L. Torner, D. Mazilu, D. Mihalache, Phys. Rev. Lett. **77**, 2455 (1996)
- 11 R. Schiek, Y. Baek, G.I. Stegeman, W. Sohler, Opt. Lett. **24**, 83 (1999)
- 12 S. Carrasco, J.P. Torres, D. Antigas, L. Torner, Opt. Commun. **192**, 347 (2001)
- 13 P. Pioger, V. Couderc, L. Lefort, A. Barthelemy, F. Baronio, C. De Angelis, Y. Min, V. Quiring, W. Sohler, Opt. Lett. **27**, 2182 (2002)
- 14 T. Pertsch, R. Iwanow, R. Schiek, G.I. Stegeman, U. Peschel, F. Lederer, Y.H. Min, W. Sohler, Opt. Lett. **30**, 1177 (2005)